OXFORD UNIVERSITY PRESS

Journal of Occupational Health, 2024, **66**(1), uiae019
https://doi.org/10.1093/JOCCUH/uiae019
Advance access publication date 16 April 2024
Original Article

Subchronic toxicity study of indium-tin oxide nanoparticles following intratracheal administration into the lungs of rats

Nagisa Matsumura[1], Yu-ki Tanaka[2], Yasumitsu Ogra[2], Kazunori Koga[3], Masaharu Shiratani[3], Kasuke Nagano[4] and Akiyo Tanaka[1,*]

[1]Environmental Health, Graduate School of Medical Sciences, Kyushu University, Fukuoka, Japan
[2]Toxicology and Environmental Health, Graduate School of Pharmaceutical Sciences, Chiba University, Chiba, Japan
[3]Department of Electronics, Faculty of Information Science and Electrical Engineering, Kyushu University, Fukuoka, Japan
[4]Nagano Toxicologic-Pathology Consulting, Hadano, Japan
*Corresponding author: Akiyo Tanaka, (tanaka.akiyo.560@m.kyushu-u.ac.jp).

Abstract

Objectives: We aimed to analyze the subchronic toxicity and tissue distribution of indium after the intratracheal administration of indium-tin oxide nanoparticles (ITO NPs) to the lungs of rats.
Methods: Male Wistar rats were administered a single intratracheal dose of 10 or 20 mg In/kg body weight (BW) of ITO NPs. The control rats received only an intratracheal dose of distilled water. A subset of rats was periodically euthanized throughout the study from 1 to 20 weeks after administration. Indium concentrations in the serum, lungs, mediastinal lymph nodes, kidneys, liver, and spleen as well as pathological changes in the lungs and kidneys were determined. Additionally, the distribution of ionic indium and indium NPs in the kidneys was analyzed using laser ablation-inductively coupled plasma mass spectrometry.
Results: Indium concentrations in the lungs of the 2 ITO NP groups gradually decreased over the 20-week observation period. Conversely, the indium concentrations in the mediastinal lymph nodes of the 2 ITO groups increased and were several hundred times higher than those in the kidneys, spleen, and liver. Pulmonary and renal toxicities were observed histopathologically in both the ITO groups. Both indium NPs and ionic indium were detected in the kidneys, and their distributions were similar to the strong indium signals detected at the sites of inflammatory cell infiltration and tubular epithelial cells.
Conclusions: Our results demonstrate that intratracheal administration of 10 or 20 mg In/kg BW of ITO NPs in male rats produces pulmonary and renal toxicities.

Key points
What is already known on this topic: To date, epidemiological studies and animal experiments have shown that the inhalation of indium tin oxide (ITO) grinding particles causes lung disorders, such as interstitial pneumonia and emphysema. Recently, ITO nanoparticles (ITO NPs) have been used in the industry as raw materials for ITO ink supplied for flat panels; however, only few reports are available on the health effects of ITO NPs, including organ distribution and organ damage. As ITO NPs have a smaller particle size than ITO ground particles, we hypothesized that they would be more likely to be deposited in internal organs and cause damage to organs other than the lungs.
What this study adds: Severe kidney and lung damage was observed following intratracheal administration of ITO NPs in rats. Furthermore, NPs, including indium, were deposited in the tubular epithelium and interstitial areas of the kidney, where severe inflammation had developed. This study found that indium-containing NPs were deposited in organs other than lungs. In addition to the indium ions eluted from ITO nanoparticles inhaled through the respiratory tract, some were also deposited as particles in the organs through systemic circulation.
How this study might affect research, practice, or policy: In Japan, only lung damage is attracting attention as an injury caused by the inhalation of ITO particles; however, the possibility of kidney damage cannot be denied. In the future, workplace medical examinations must consider renal disorders in the industrial health field.

Keywords: indium-tin oxide nanoparticle; pulmonary toxicity; renal toxicity; tissue indium distribution; rat.

Introduction

Indium-tin oxide (ITO) is a sintered alloy containing 90% indium oxide and 10% tin oxide. Thin-film ITO coatings are primarily used for electrical conductivity in various flat-panel displays, most commonly liquid crystal panels.[1] Although a steady demand exists for ITO owing to the growing smart device market, previous studies have shown that ITO is the causative agent of occupational lung diseases. The first case of interstitial pneumonia caused by occupational exposure to ITO was reported in 2003.[2] Since then, a series of lung injuries have been reported among ITO-exposed workers, including several critical cases that resulted

Received: November 15, 2023. **Revised:** February 15, 2024. **Accepted:** March 29, 2024

in lung transplantation or death.[3-8] Epidemiological studies on ITO-exposed workers have revealed an association between ITO exposure and indium lung disease, which is characterized by interstitial or emphysematous changes. Higher serum indium concentrations are associated with a higher risk of lung damage.[9-12] Moreover, ITO exposure may be a risk factor for lung cancer.[13] Previous studies on animals have shown that ITO exposure causes lung inflammation[14-17] and increases the incidence of lung malignancies.[18]

Recently, ITO nanoparticles (NPs) have attracted considerable attention. ITO is typically deposited on substrates by sputtering; however, large amounts of ITO are wasted during this process. In contrast, the method of printing ITO nanoinks on substrates is less wasteful; therefore, current materials research has focused on the synthesis of ITO NPs and printing methods using ITO nanoinks.[19] Furthermore, recently developed ITO NP thin films with high transparency, microwave transmission, and solar heat shielding can be applied to windows in buildings and automobiles.[20] In addition to the widespread use of ITO NPs, studies on the size of dust generated in ITO target manufacturing plants have detected indium-containing NPs.[21] Therefore, understanding whether exposure to ITO NPs causes the same or greater health hazards than exposure to ground ITO powder is important.

Generally, small-diameter particles reach deeper into the lungs and cause severe lung damage. Several studies in which ITO NPs were administered to animals have revealed that ITO NPs cause lung damage similar to that in indium lung[22-24]; and Qu et al[22] showed that smaller particles require less exposure to cause lung damage than larger particles. In vitro studies using human lung epithelial cells have shown that ITO NPs are absorbed by the cells and cause DNA damage.[25,26] Additionally, when animals are administered ITO NPs, indium is deposited not only in the lungs but also in other organs and can damage distal organs, such as the kidney and liver.[22,23] However, few studies have conducted detailed examinations of organs other than lungs.

In this study, we aimed to clarify the subchronic toxicity of indium in the lungs and other organs after intratracheal administration of ITO NPs in rats. These results indicate that indium is deposited in organs throughout the body, causing significant damage to the lungs and other organs, particularly the kidneys.

Materials and methods

Animals

Sixty-three 6-week-old male Wistar rats from the colony of Japan SLC, Inc. (Shizuoka, Japan) were purchased and housed under temperature conditions of between 22°C and 25°C. The rats were maintained under a cycle of 12-hour lighting, within a specific-pathogen-free laboratory room at the Laboratory of Animal Experiments, Graduate School of Medical Sciences, Kyushu University. The rats were provided a commercial diet and water ad libitum. Intratracheal administration was conducted in 8-week-old rats after an acclimatization period of 2 weeks. Experiments were conducted in accordance with the Regulations for Animal Experiments at Kyushu University (A20-020-0) and the Basic Policy on the Conduct of Animal Experiments at the Research Institutes of the Ministry of Education, Culture, Sports, Science, and Technology Public Notice No. 71, 2006, Japan.

ITO nanoparticle preparation

ITO NPs with a particle size of 18 nm (scanning electron microscopy) and 20 wt% H_2O were purchased from Sigma-Aldrich Japan, Tokyo, Japan. The mean secondary particle size of ITO NPs in the distilled water dispersion was 131.5 nm, measured using the dynamic light scattering particle size analyzer (Nanotrac WAVE II EX150; MicrotracBEL Corp., Osaka, Japan) after pretreatment with ultrasonic homogenizer (US-150E; NIHONSEIKI KAISHA Ltd, Tokyo, Japan) at 150 W for 3 minutes.

Experimental design

In preliminary experiments, 10 and 30 mg In/kg body weight (BW) ITO NPs were intratracheally administered to rats. Some rats in the 30 mg In/kg BW group became severely debilitated, and 5 of the 11 rats died of severe chronic nephropathy within 20 weeks. Therefore, in this experiment, the ITO NP dose was set at 20 mg In/kg BW, and half of the dose was set at 10 mg In/kg BW.

The rats, with a mean ± SE weight of 187.6 ± 0.8 g, were randomly divided into 3 groups: control group ($n = 20$), a group treated with a dose of 10 mg In/kg BW of ITO NPs (ITO 10 mg group, $n = 20$), and a group treated with a dose of 20 mg In/kg BW of ITO NPs (ITO 20 mg group, $n = 23$). No significant differences in BW were observed among the groups at the start of the experiment. The ITO NPs were diluted with sterile distilled water before each administration. Rats in the ITO 10 mg and ITO 20 mg groups received a single intratracheal administration of ITO NPs at doses of 10 and 20 mg In/kg BW, respectively. The control group received 1 mL/kg of distilled water via a single intratracheal administration. Rats were anesthetized with isoflurane at the time of administration.

Five to 7 surviving rats in each group were euthanized using sevoflurane at 1, 4, 12, or 20 weeks after administration, and then autopsied. Blood was collected from the posterior vena cava, and serum was separated by centrifugation. Serum was stored at −80°C to measure indium concentration. The resected internal organs (the lungs, mediastinal lymph nodes, kidneys, liver, and spleen) were weighed. Portions of the obtained fresh organs were stored at −80°C to measure the indium concentration. Other organs were fixed in 10% neutral-buffered formalin for subsequent evaluation of histopathological changes and detection of ITO NPs.

Determination of indium concentrations

The serum was digested with 4 mL of 68% ultrapure nitric acid (TAMAPURE-AA-100; Tama Chemicals Co., Ltd, Kanagawa, Japan) and 2 mL of 35% ultrapure hydrogen peroxide (TAMAPURE-AA-100) using a microwave digestion apparatus (MultiwavePRO; Anton Paar Japan K.K., Tokyo, Japan). The lungs, mediastinal lymph nodes, kidneys, liver, and spleen were digested with 6 mL nitric acid and hydrogen peroxide (0.5 mL) using a microwave digestion apparatus. The digested samples were diluted to 20 mL with ultrapure water, and rhodium (Rh) solution was added as an internal standard. The final Rh concentration was set at 0.5 μg/L. All samples were analyzed by inductively coupled plasma mass spectrometry (ICP-MS 7500c; Agilent Technologies Japan, Ltd, Tokyo, Japan) at the Center of Advanced Instrumental Analysis, Kyushu University. The lower limits of quantitation (QL) of indium were 0.0001 μg/mL for serum, 0.001 μg/g for lungs, 0.01 μg/g for lymph nodes, and 0.0012 μg/g for the kidney, liver, and spleen. If the indium concentration was below the QL, half the QL value was used for statistical analyses.

Histopathological evaluation

The organs in 10% neutral-buffered formalin were processed in paraffin. Specimens were cut at a thickness of 4 μm and each section was stained with hematoxylin-eosin (HE). Selected chronic nephropathy sections from the kidneys were stained with periodic acid-Schiff (PAS). The sections were examined under a light

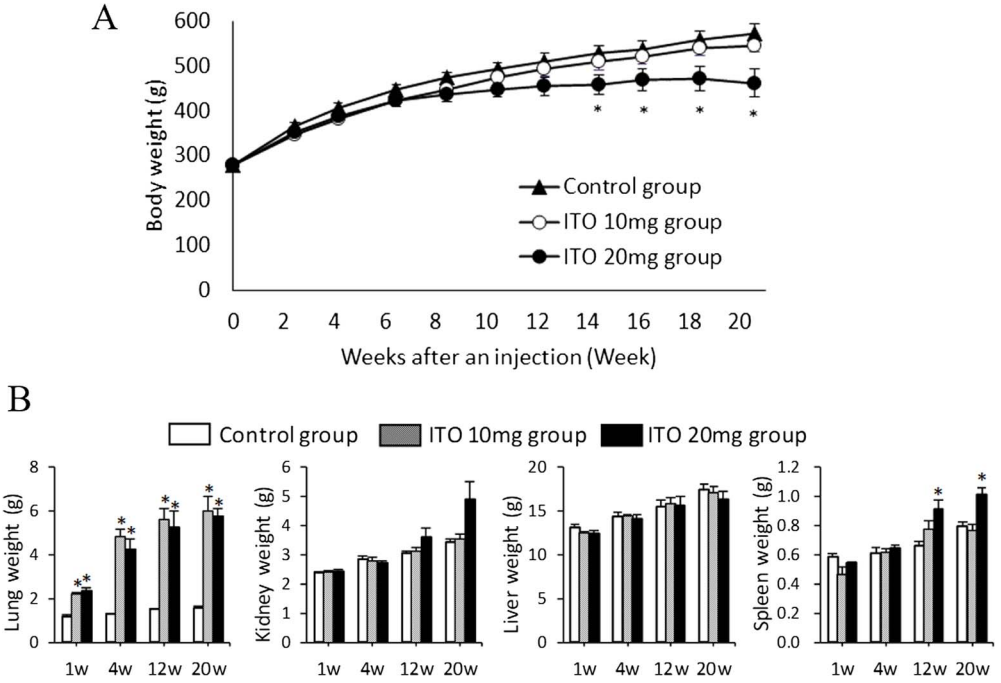

Figure 1. Changes in body and organ weights. (A) Changes in body weight during the observation period. The results are shown as the mean ± SE of rats euthanized at Week 20. (B) Changes in organ weight after administration. The results are shown as the mean ± SE of organ weights of rats euthanized at each time point after administration. ∗Denotes significant difference compared with the control group ($P < .05$).

microscope. Histopathological findings in the organs were scored as present or absent. If absent, the findings were considered negative. The severity of the organ lesions was graded on a 4-item scale ranging from slight to severe, indicating the approximate fraction of the structure judged to be involved (slight = 1%-10%, mild = 11%-24%, moderate = 25%-50%, and severe = 51%-100%). According to the above lesion classification, the extent of the lesion was scored from 0 to 4, with 0 being no lesions, 1 being slight, 2 being mild, 3 being moderate, and 4 being severe, and then semiquantified. The average value of each lesion was rounded off, and 0.1 to 0.4 was evaluated as "−," 0.5 to 1.4 as "±", 1.5 to 2.4 as "+", 2.5 to 3.4 as "2+", and 3.5 or higher as "3+."

In situ elemental analysis through laser ablation inductively coupled plasma mass spectrometry

One rat in the ITO 20 mg group was euthanized at Week 20, and its kidney was used to measure the indium concentration by laser ablation inductively coupled plasma mass spectrometry (LA-ICP-MS). Paraffin-embedded and HE-stained tissue specimens were subjected to LA-ICP-MS analysis, and 2 different in situ elemental analyses were conducted: (1) The distributions of the total amounts of elements were obtained using quadrupole-based ICP-MS (Agilent 8800 ICP-MS/MS; Agilent Technologies, Tokyo, Japan) coupled with a laser ablation system (NWR213; ESI, Fremont, CA, USA). The signal intensities of ^{57}Fe and ^{115}In were monitored at a dwell time of 100 ms by raster scanning. Elemental distributions were visualized using iQuant2 software.[27] (2) Distributions of indium ions and indium-containing NPs were separately obtained in fast time-resolved analysis using quadrupole-based ICP-MS (Agilent 8900 ICP-MS/MS; Agilent Technologies) coupled with an NWR213. The signal intensity of ^{115}In was monitored with a dwell time of 0.1 ms. Subsequently, the signal intensities were analyzed using software developed by Yamashita et al.[28]

Statistical analysis

Data are expressed as mean ± SE. Differences between the control and ITO groups were evaluated using the Welch t test with a closed testing procedure. Comparisons were made with the control group, starting with the high-dose group, until no significant difference was found. As it was known from previous experiments that the difference between the control and ITO groups in body and organ weights gradually increased, the tests started at Week 20 and continued retrospectively until no significant differences were found. For indium concentrations, P values were multiplied by 4 after performing closed-procedure t tests between the control and ITO groups at all time points. In all statistical comparisons, a P value $<.05$ was used to determine significant differences. All statistical analyses were conducted using EZR (Saitama Medical Center, Jichi Medical University, Saitama, Japan), a graphical user interface for R (R Foundation for Statistical Computing, Vienna, Austria).

Results

Body and organ weights

None of the rats died during the intratracheal administration or the observation period. Changes in BW throughout the observation period are shown in Figure 1A for the 17 animals (5, 7, and 5 in the 10 mg ITO, 20 mg ITO, and control groups, respectively) observed until 20 weeks after administration. Mean BWs (±SE) at Week 20 were 546.2 ± 15.2, 461.7 ± 32.0, and 572.2 ± 20.4 g in the ITO 10 mg, ITO 20 mg, and control groups, respectively. The increases in the BWs of the control and ITO 10 mg groups showed similar trends, whereas the weight gain in the ITO 20 mg group was slower and the BW of the ITO 20 mg group was significantly lower than that of the control group after Week 14. No systemic signs, such as respiratory distress, dermatological abnormalities, or behavioral or neurological disorders, appeared during the observation period in any group.

Table 1. Indium concentrations in the serum and organs in weeks after an instillation.[a]

Organ	Group	Concentration (no. of rats examined)			
		Week 1	Week 4	Week 12	Week 20
Lung, μg/g	ITO 10 mg	1017 ± 100* (5)	316 ± 53* (5)	212 ± 75 (5)	86 ± 16* (5)
	ITO 20 mg	1342 ± 337* (5)	420 ± 116* (5)	343 ± 97* (6)	287 ± 31* (7)
Mediastinal lymph	ITO 10 mg	276 ± 98 (4)	622 ± 120 (5)	963 ± 289 (5)	1689 ± 163 (5)
node, μg/g	ITO 20 mg	401 ± 135 (5)	961 ± 131 (5)	1249 ± 362 (6)	3823 ± 926 (6)
Kidney, μg/g	ITO 10 mg	0.79 ± 0.17* (5)	1.80 ± 0.21* (5)	4.25 ± 0.66 (5)	4.07 ± 1.2 (5)
	ITO 20 mg	1.81 ± 0.44* (5)	4.49 ± 1.26* (5)	21.54 ± 8.5 (6)	17.1 ± 2.92* (7)
Spleen, μg/g	ITO 10 mg	0.40 ± 0.10* (5)	0.99 ± 0.08 (5)	4.35 ± 0.77* (5)	4.83 ± 0.84* (5)
	ITO 20 mg	0.77 ± 0.18* (5)	2.91 ± 0.88 (5)	10.51 ± 1.76* (6)	9.05 ± 1.34* (7)
Liver, μg/g	ITO 10 mg	0.28 ± 0.05* (5)	0.74 ± 0.08* (5)	1.42 ± 0.19* (5)	1.28 ± 0.43 (5)
	ITO 20 mg	0.75 ± 0.16* (5)	1.76 ± 0.46* (5)	5.65 ± 1.08* (6)	3.94 ± 0.57* (7)
Serum, μg/mL	ITO 10 mg	0.11 ± 0.03* (5)	0.17 ± 0.02 (5)	0.27 ± 0.04* (5)	0.14 ± 0.04* (5)
	ITO 20 mg	0.26 ± 0.07* (5)	0.43 ± 0.13 (5)	0.4 ± 0.07* (6)	0.23 ± 0.05* (7)

Abbreviation: ITO, indium-tin oxide.
[a]The indium concentrations are shown as the mean ± SE in the serum and organs of rats euthanized at each time point after an administration. Indium concentrations in the control group were below the limit of quantitation at all the time points. *Denotes significant difference compared with that of the control group ($P < .05$).

The changes in the weights of the lungs, kidneys, liver, and spleen during the observation period are shown in Figure 1B. The lung weights in the 2 ITO groups were significantly higher than those in the control group at all time points. The spleen weights in the ITO 20 mg group were significantly higher than those in the control group at Weeks 12 and 20. No statistically significant differences were observed in kidney and liver weights between the 2 ITO groups and the control group at any time point.

Indium concentrations in serum and organs

The indium concentrations in the serum, lungs, mediastinal lymph nodes, kidneys, liver, and spleen of the 2 ITO groups and the control group during the observation period are presented in Table 1. Mediastinal lymph nodes were not sampled from any of the rats in the control group and from 1 each in the ITO 10 mg and ITO 20 mg groups at Weeks 1 and 20, respectively. Additionally, 3 out of 7 rats in the ITO 20 mg group at Week 20 had enlarged pelvic lymph nodes that could be used to measure indium concentration. However, samples from all rats, other than those in the ITO 20 mg group at Week 20, could not be obtained. Indium concentrations in each organ of the control group were below the QL at all the time points. Indium concentrations in the serum and all organs were higher in the ITO 20 mg group than in the ITO 10 mg group. In the 2 ITO groups, indium concentrations in the lungs gradually decreased during the observation period at a faster rate for the first 4 weeks and at a slower rate from Weeks 4 to 20. The half-lives of indium concentrations in the lung were 1.8 weeks from Weeks 1 to 4 and 8.5 weeks from Weeks 4 to 20 for the ITO 10 mg group, and 1.8 weeks from Weeks 1 to 4 and 29 weeks from Weeks 4 to 20 for the ITO 20 mg group. Indium concentrations in the mediastinal lymph nodes of the 2 ITO groups increased during the observation period and exceeded those in the lungs after Week 4. Furthermore, indium concentrations in the mediastinal lymph nodes were approximately 20 times higher in the ITO 10 mg group and 13 times higher in the ITO 20 mg group than in the lungs at Week 20.

The indium concentrations in the serum, kidney, liver, and spleen of the 2 ITO groups increased through Week 12 and leveled off or decreased by Week 20. At Week 20, the mean indium levels in the ITO 10 mg group were in the following descending order: mediastinal lymph nodes > lung > spleen > kidney > liver > serum, and those in the ITO 20 mg group were in the following descending order: mediastinal lymph nodes > lung > kidney > spleen > liver > serum.

In addition to the aforementioned organs, the mean indium level in the pelvic cavity lymph node ($n = 3$) was 12.9 ± 3.9 μg/g (mean ± SE) in the ITO 20 mg group at Week 20. In contrast, that in the mediastinal lymph nodes of the same 3 animals was 3825.6 ± 1957.8 μg/g.

Histological changes

Photographs and microphotographs of the lungs are shown in Figure 2. The severity of the pathological changes in the lungs is presented in Table 2. In general, the lungs of the 2 ITO groups were enlarged at all the time points. Based on the histopathological findings, diffuse foci with moderate-to-severe inflammation were present in the 2 ITO groups during the observation period. Although severe inflammatory lesions appeared at Week 1 in the ITO 20 mg group, the degree of inflammation decreased after Week 4. Within the region of the inflammatory foci, we observed infiltration of lymphocytes and neutrophils around the blood vessels and enlargement or diffuse hyperplasia of type II alveolar cells. Additionally, alveolar macrophages with an expanded cytoplasm or ITO particles were observed within the alveolar spaces. Necrosis of alveolar macrophages was observed at all time points during the observation period but was particularly severe at Week 1 in the ITO 20 mg group. Moderate exudation, including necrotic fragments, was observed within the alveolar spaces at an early stage in both the ITO groups, and the degree of exudation decreased by Week 20. Cholesterol clefts gradually manifested after Week 12 in both the ITO groups. Expansion of the alveolar spaces was slight to mild in both ITO groups at all observation points.

Photographs and microphotographs of the kidneys are shown in Figure 3. The severity of chronic nephropathy in the kidneys is shown in Table 2. Considering the gross findings, some kidneys in the ITO 20 mg group were enlarged, had a rough surface, and turned greenish-brown after Week 12, whereas the kidney surface was dark brown in the ITO 10 mg and control groups at all time points. Foci were mild-to-moderate in the ITO 20 mg group and slight in the ITO 10 mg group; Chronic nephropathy was observed after Week 12. Within the chronic nephropathy foci, tubule atrophy, tubal lumen dilation, basophilic tubules,

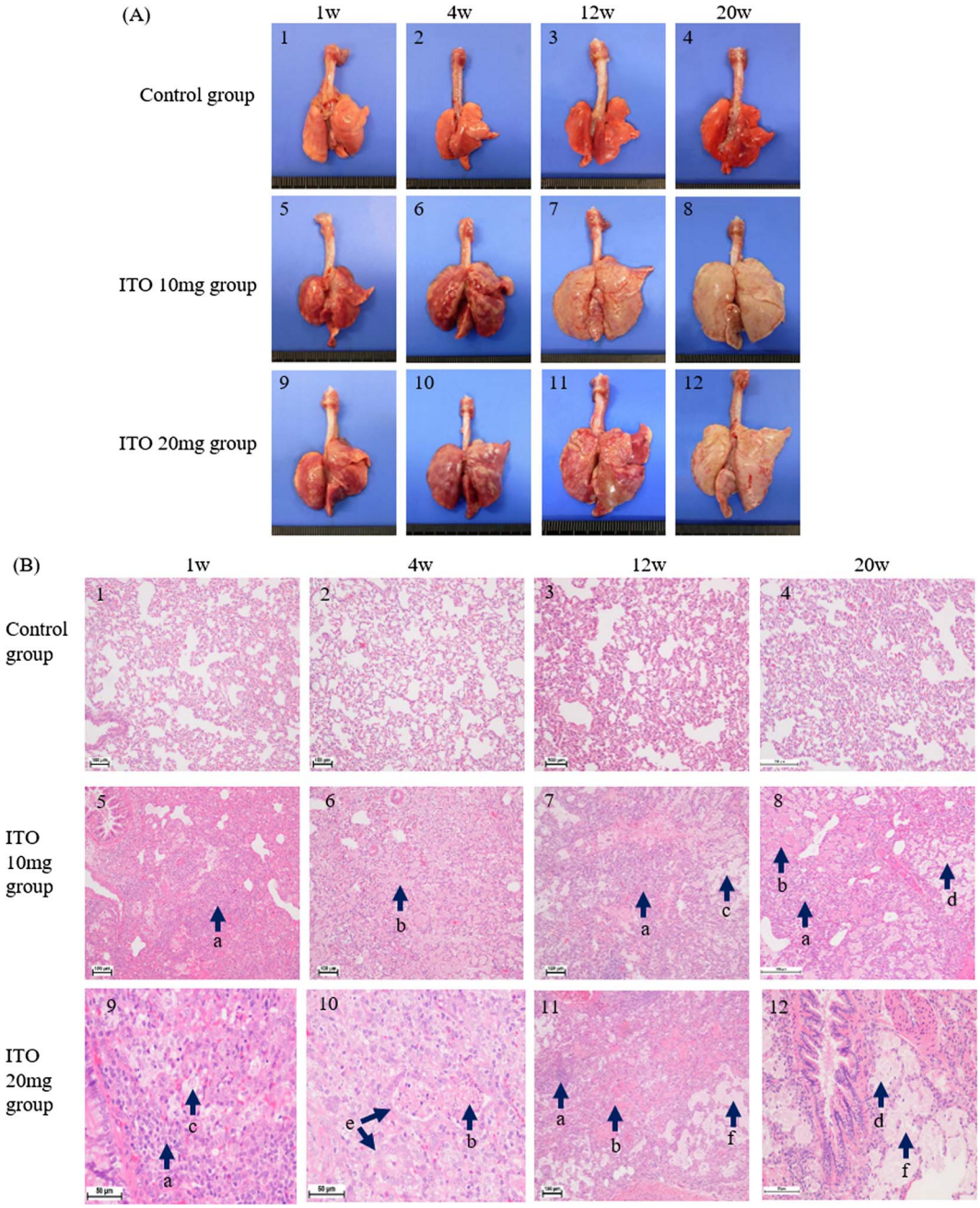

Figure 2. Pathological changes in the lungs in each group from Week 1 to 20. (A) Macroscopic photographs in the lungs. (B) Histopathological images in the lungs: (1, 2, 3, and 4) photographs of the control group; (5, 6, 7, and 8) photographs of the ITO 10 mg group; (9, 10, 11, and 12) photographs of the ITO 20 mg group. As shown in (A), in the ITO 10 mg group, the lung surface was reddish-brown, rough, and slightly indurated at Weeks 1 (5) and 4 (6); it was grayish-pink in color and moderately swollen at Weeks 12 (7) and 20 (8). In the ITO 20 mg group, the lung surface was reddish-brown, rough, and slightly indurated at Weeks 1 (9), 4 (10), and 12 (11); it was grayish-pink in color and moderately swollen at Week 20 (12). As shown in (B), in the photographs of rats in the control group, the pulmonary tissue structure was normal (1, 2, 3, and 4). In the photographs of the rats in the ITO 10 mg group, extensive inflammation (a), exudation of necrotic debris from alveolar macrophages in the alveolar space (b), alveolar macrophage necrosis (c), and a slight cholesterol cleft (d) were evident. In the photographs of rats in the ITO 20 mg group, extensive inflammation (a), exudation of necrotic debris from alveolar macrophages in the alveolar space (b), alveolar macrophage necrosis (c), exudation of necrotic debris from alveolar macrophages in the alveolar space (d), enlargement or diffuse hyperplasia of alveolar cell type II (e), and expansion of the alveolar space (f) were evident.

hyaline casts, and hyaline droplet degeneration were observed. In addition, we observed inflammatory cell infiltration into the stroma, stromal expansion, and glomerular atrophy. PAS staining of the kidneys revealed positive hyaline casts in the renal tubules and granules in the cytoplasm of renal tubular epithelial cells in the ITO 20 mg group at Week 20. The degree of severity increased from Week 12 to 20.

Characteristic pathological findings were not observed in organs other than the lungs and kidneys compared with those in the control group.

LA-ICP-MS analysis of the kidney

One rat kidney in the ITO 20 mg group was separately analyzed using LA-ICP-MS for indium NPs and ionic indium, and both

Table 2. Pathological changes

Pathological changes in the lungs of rats euthanized at each time point after administration	Group	Weeks after an instillation in the lungs and kidneys.[a]			
		Week 1	Week 4	Week 12	Week 20
Inflammatory response	ITO 10 mg	2+	2+	2+	2+
	ITO 20 mg	3+	2+	2+	1+
	Control	–	–	–	–
Alveolar macrophage necrosis	ITO 10 mg	2+	2+	2+	2+
	ITO 20 mg	3+	2+	2+	2+
	Control	–	–	–	–
Exudation with necrotic fragments in alveolar spaces	ITO 10 mg	2+	2+	2+	1+
	ITO 20 mg	2+	2+	2+	1+
	Control	–	–	–	–
Cholesterol clefts	ITO 10 mg	–	–	±	±
	ITO 20 mg	–	–	±	±
	Control	–	–	–	–
Expansion of alveolar spaces	ITO 10 mg	±	±	1+	1+
	ITO 20 mg	1+	±	1+	±
	Control	–	–	–	–
Severity of chronic nephropathy in rats euthanized at each time point	ITO 10 mg	–	–	±	±
	ITO 20 mg	–	–	1+	2+
	Control	–	–	–	–

Abbreviation: ITO, indium-tin oxide.
[a]The severity of the lung or kidney lesions was categorized into 5 grades. –: negative; ±: slight; 1+: mild; 2+: moderate; 3+: severe.

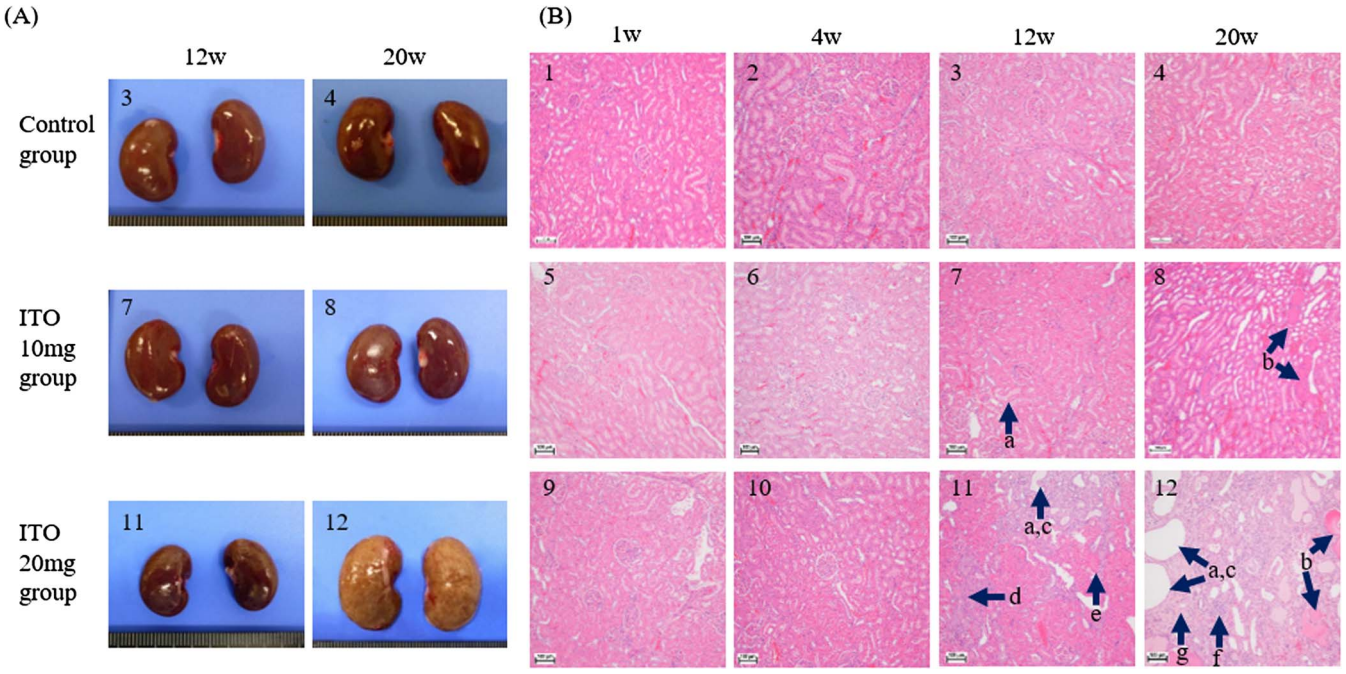

Figure 3. Pathological changes in the kidneys in each group from Week 1 to 20. (A) Macroscopic photographs in the kidneys. (B) Histopathological images of kidneys: (1, 2, 3, and 4) photographs of the control group; (5, 6, 7, and 8) photographs of the ITO 10 mg group; (9, 10, 11, and 12) photographs of the ITO 20 mg group. No macroscopic changes were observed in any of the groups at Weeks 1 or 4 (data not shown). As shown in (A), the surfaces of the control group were dark brown and smooth at Weeks 12 (3) and 20 (4), respectively. In the ITO 10 mg group, the kidney surface was dark brown and smooth at Weeks 12 (7) and 20 (8). In the ITO 20 mg group, the kidney surface was dark brown and smooth at Week 12 (11), and it was enlarged with a rough, gray-green surface at Week 20 (12). As shown in (B), in the photographs of rats in the control group, the kidney tissue structure was normal (1, 2, 3, and 4). In the photographs of the rats in the ITO 10 mg group, slight tubal lumen dilation (a) and hyaline casts (b) were evident. In the photographs of rats in the ITO 20 mg group, mild to moderate lesions of tubal lumen dilation (a), hyaline casts (b), tubal atrophy (c), basophilic tubules (d), hyaline droplet degeneration (e), interstitial inflammatory cell infiltration (f), and interstitial fibrosis (g) were observed.

signals were detected. The indium NP signal was particularly strong at sites of inflammatory cell infiltration and tubular epithelial cells and was barely detected in the glomeruli (Figure 4A-F). The resulting total element image shows very similar distributions of indium and iron (Figure 4G-I). Indium and iron signals were stronger in tubular epithelial cells, whereas indium- and iron-rich cells were found at sites of cellular infiltration into the stroma.

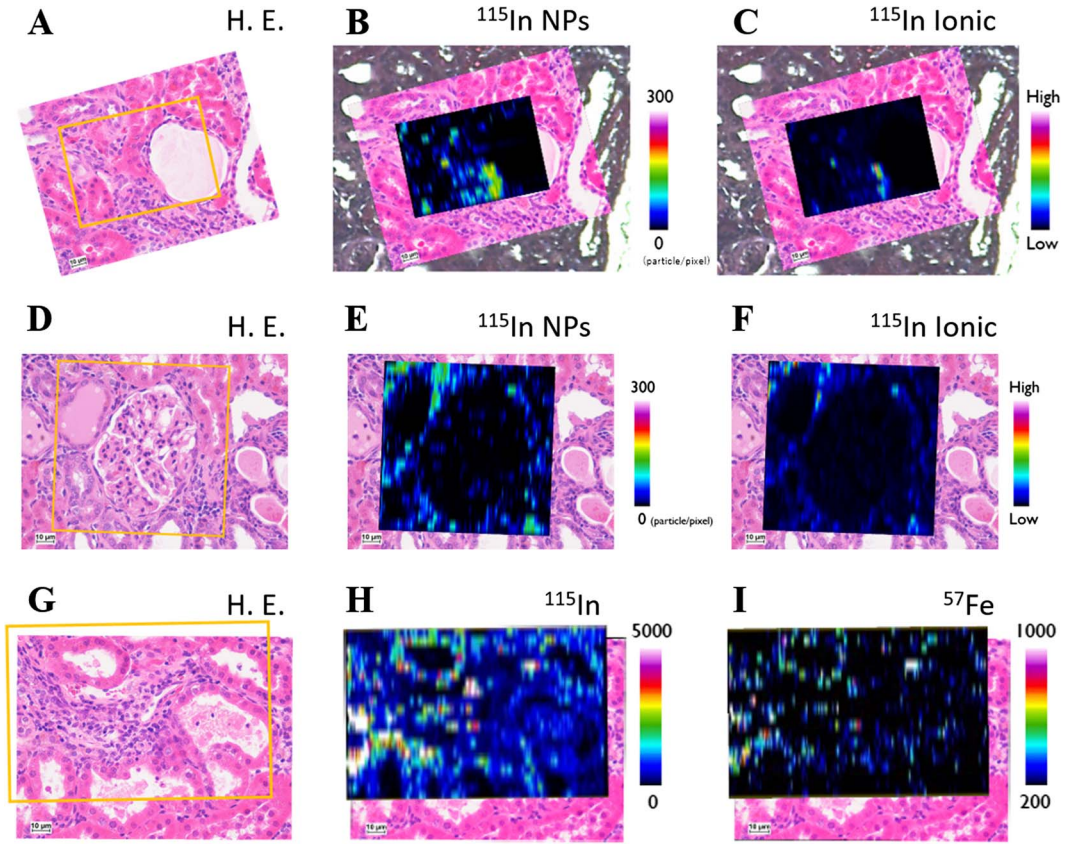

Figure 4. Laser ablation inductively coupled plasma mass spectrometry (LA-ICP-MS) image of the kidney of a rat in the ITO 20 mg group at Week 20. (A) and (D) photomicrographs of kidneys stained with hematoxylin and eosin. The yellow-framed area was analyzed using LA-ICP-MS for indium with 2 properties. The resulting distributions of the elements were as follows: (B) and (E) indium nanoparticles; (C) and (F) ionic indium. (G) Photomicrograph of kidneys stained with hematoxylin and eosin. The yellow area was analyzed using LA-ICP-MS for total amounts of elements. The resulting distributions for the elements were as follows: (H) indium and (I) iron.

Discussion

In our study, we revealed that intratracheal administration of ITO NPs in rats induced pulmonary and renal toxicities. A single intratracheal administration of ITO NPs in rats caused inflammatory responses in the lungs, necrosis of alveolar macrophages, and exudation of necrotic fragments into the alveoli 1 week after administration. These lesions were similar to those observed in our previous experiments in hamsters exposed to non-nanosized ITO particles.[16] However, although lung injury worsened over time in our previous experiments, the present administration of ITO NPs produced a severe inflammatory reaction as early as 1 week after administration, and its severity gradually decreased. Indium concentrations in the lungs gradually decreased during the observation period after administration. In contrast, the indium concentrations in the mediastinal lymph nodes increased rapidly during the observation period, reaching several hundred times higher than those in the kidneys, spleen, and liver. The number of mediastinal lymph nodes in the 2 ITO groups increased as early as 1 week after administration. Moreover, lymph nodes in the pelvic cavity were enlarged in some rats in the ITO 20 mg group at Week 20. These results suggest that ITO NPs with small particle sizes have a strong injurious effect on the lungs early in the observation period, whereas their clearance from the lungs is rapid compared with that of non-nanosized ITO NPs, and repair following lung inflammation caused by ITO NPs is relatively good. The lymphatic system plays a major role in the clearance of ITO NPs from the lungs.

Notably, we observed damage to the kidneys of rats intratracheally administered ITO NPs. After 12 weeks, chronic nephropathy was particularly pronounced in the high-dose ITO-NP group. Although the kidney weight of the ITO 20 mg group at Week 20 was not significantly different ($P = .0603$), it showed an increasing trend, and the surface was macroscopically rough and swollen (Figure 3), suggesting a strong effect of the ITO particles on the kidneys. In conjunction with the appearance of chronic nephropathy, renal indium concentrations increased remarkably at 12 weeks, with a greater degree of renal indium deposition in the ITO 20 mg group than in the ITO 10 mg group. These findings suggest that the kidney is susceptible to subchronic toxic effects caused by ITO NPs and that indium can easily accumulate. LA-ICP-MS analysis was performed to visualize the distribution of indium in the kidneys. By separately analyzing indium NPs and ions, we detected indium NPs in the kidneys. Ionic indium has a strong affinity for transferrin and is known to bind to it in the serum[29,30]; however the detection of indium NPs in the kidney, a remote organ, suggests that indium NPs circulate in the body not only in the ionic form bound to transferrin, but also in the NP form. In addition, the distributions of indium NPs and indium ions were similar, with strong signals detected at the sites of inflammatory cell infiltration. Although previous studies have suggested that ITO NPs may be involved in renal damage,[22,23] this study revealed that ITO NPs, in addition to ionized indium, strongly contribute to the development of renal damage.

Huaux et al[31] reported that in the lungs, interstitial macrophages release ionic indium when they phagocytose ITO

particles, and the released ionic indium binds to transferrin. In the LA-ICP-MS images, high indium signals were observed at the sites of inflammatory cell infiltration into the stroma. Macrophages in the renal interstitium may phagocytose ITO NPs and subsequently release ionic indium into the kidneys, similar to the process in the lungs. The distributions of indium and iron were similar in the resulting total-element images. Ionic indium is transported into the blood and binds to transferrin. Although transferrin is primarily an iron-binding protein, it can bind to other metal ions entering the body, because transferrin in human serum is only saturated with approximately 30% iron.[29] Therefore, ionic indium is thought to bind to excess binding sites and behave in the same manner as iron, which is supported by the results of the present study. Tubular epithelial cells showed a high total indium signal. This is consistent with a report by Wood and Fowler,[32] indicating that indium is selectively localized in the proximal tubules of the kidney. Moreover, in an experiment in which indium chloride and indium hydroxide were administered to mice through the tail vein, acute proximal tubule necrosis was observed several days after administration, whereas no changes were observed in the other tubules or glomeruli.[33] In our study, histological lesions in the kidney were found in the tubules, stroma, and glomeruli; however, indium deposition was limited to tubular epithelial cells and sites of cellular infiltration in the stroma and was rarely observed in the glomeruli. These results suggest that indium is first taken up by the tubular epithelium, causing an inflammatory response due to its toxicity, and the lesions then spread to the glomerulus. To date, no case reports or epidemiological studies on kidney damage have been reported in indium-exposed workers,[2-5,7,9-11] but the results of our study suggest that the occurrence of kidney damage in indium-exposed workers requires more attention.

Our study has several limitations. The number of rats in each group used at each time point was small, ranging from 5 to 7. Additionally, although only male rats were used, because the incidence of chronic progressive nephropathy, which is common in rats, is higher in males than in females,[34] further studies are required to investigate whether female rats show the same findings as those observed in our study. Further studies with larger sample sizes are required to confirm the role of ITO NPs in kidney damage. Additionally, although only 1 type of ITO NPs was used in this study, future studies are needed to investigate whether different particle sizes of ITO NPs have different biological effects, as several studies have shown that different particle sizes of ITO NPs exert different biological effects.[22,25]

To date, no data are available concerning the health effects of workers engaged in handling ITO NPs. However, it is expected that indium will be depleted in the future owing to the increased production of solar cells, and it is assumed that indium will be recovered from the large number of solar cells used. Based on the results of the present study, sufficient caution must be taken when recovering the indium and disposing of products containing ITO.

Acknowledgments

We thank Mrs Etsuko Shibata for technical assistance. We also would like to thank Editage (www.editage.jp) for the English language editing.

These experiments were conducted in accordance with the Regulations for Animal Experiments at Kyushu University and the Basic Policy on the Conduct of Animal Experiments at Research Institutes from the Ministry of Education, Culture, Sports, Science, and Technology Public Notice No. 71, 2006, Japan.

Author contributions

A.T. conceived and designed the study. A.T. and N.M. conducted animal experiments. K.K. and M.S. performed the particle analyses. N.M. analyzed indium concentrations. A.T. and K.N. conducted the pathological evaluations. Y.T. and Y.O. conducted LA-ICP-MS analysis. A draft of the manuscript was written by N.M. and critically revised by A.T. All authors approved the final version of the manuscript.

Funding

This study was funded, in part, by a Grant-in-Aid for Scientific Research (B) (16H05257) from the Ministry of Education, Culture, Sports, Science, and Technology of Japan.

Conflicts of interest

None declared.

Data availability

The data that support the findings of this study are available from the corresponding author upon reasonable request.

References

1. *US Geological Survey. Mineral commodity summaries 2022*. Accessed December 21, 2022. http://pubs.er.usgs.gov/publication/mcs2022
2. Homma T, Ueno T, Sekizawa K, Tanaka A, Hirata M. Interstitial pneumonia developed in a worker dealing with particles containing indium-tin oxide. *J Occup Health*. 2003;**45**(3):137-139. https://doi.org/10.1539/joh.45.137
3. Homma S, Miyamoto A, Sakamoto S, Kishi K, Motoi N, Yoshimura K. Pulmonary fibrosis in an individual occupationally exposed to inhaled indium-tin oxide. *Eur Respir J*. 2005;**25**(1):200-204. https://doi.org/10.1183/09031936.04.10012704
4. Cummings KJ, Donat WE, Ettensohn DB, Roggli VL, Ingram P, Kreiss K. Pulmonary alveolar proteinosis in workers at an indium processing facility. *Am J Respir Crit Care Med*. 2010;**181**(5):458-464. https://doi.org/10.1164/rccm.200907-1022CR
5. Xiao YL, Cai HR, Wang YH, Meng FQ, Zhang DP. Pulmonary alveolar proteinosis in an indium-processing worker. *Chin Med J*. 2010;**123**(10):1347-1350
6. Nakano M, Hirata M, Hamasaki M *et al.* Indium kinetics in an indium exposed worker before and after bilateral lung transplantation. *J Occup Health*. 2020;**62**(1):e12165. https://doi.org/10.1002/1348-9585.12165
7. Tsao YC, Fan HY, Luo JJ. Case reports of indium lung disease in Taiwan. *J Formos Med Assoc*. 2021;**120**(2):893-898. https://doi.org/10.1016/j.jfma.2020.08.009
8. Inoue C, Ohkouchi S, Chonan T *et al.* A case report of indium lung with progressive emphysema and fibrosis underwent lung unilateral transplantation 20 years after the end of the exposure. *Diagn Pathol*. 2023;**18**(1):10. https://doi.org/10.1186/s13000-023-01303-1
9. Chonan T, Taguchi O, Omae K. Interstitial pulmonary disorders in indium-processing workers. *Eur Respir J*. 2007;**29**(2):317-324. https://doi.org/10.1183/09031936.00020306
10. Hamaguchi T, Omae K, Takebayashi T *et al.* Exposure to hardly soluble indium compounds in ITO production and recycling

plants is a new risk for interstitial lung damage. *Occup Environ Med*. 2008;**65**(1):51-55. https://doi.org/10.1136/oem.2006.029124
11. Nakano M, Omae K, Tanaka A *et al.* Causal relationship between indium compound inhalation and effects on the lungs. *J Occup Health*. 2009;**51**(6):513-521. https://doi.org/10.1539/joh.l9077
12. Nakano M, Omae K, Uchida K *et al.* Five-year cohort study: emphysematous progression of indium-exposed workers. *Chest*. 2014;**146**(5):1166-1175. https://doi.org/10.1378/chest.13-2484
13. Nakano M, Omae K, Tanaka A, Hirata M. Possibility of lung cancer risk in indium-exposed workers: an 11-year multicenter cohort study. *J Occup Health*. 2019;**61**(3):251-256. https://doi.org/10.1002/1348-9585.12050
14. Tanaka A, Hirata M, Omura M *et al.* Pulmonary toxicity of indium-tin oxide and indium phosphide after intratracheal instillations into the lung of hamsters. *J Occup Health*. 2002;**44**(2):99-102. https://doi.org/10.1539/joh.44.99
15. Lison D, Laloy J, Corazzari I *et al.* Sintered indium-tin-oxide (ITO) particles: a new pneumotoxic entity. *Toxicol Sci*. 2009;**108**(2):472-481. https://doi.org/10.1093/toxsci/kfp014
16. Tanaka A, Hirata M, Homma T, Kiyohara Y. Chronic pulmonary toxicity study of indium-tin oxide and indium oxide following intratracheal instillations into the lungs of hamsters. *J Occup Health*. 2010;**52**(1):14-22. https://doi.org/10.1539/joh.l9097
17. Nagano K, Gotoh K, Kasai T *et al.* Two- and 13-week inhalation toxicities of indium-tin oxide and indium oxide in rats. *J Occup Health*. 2011;**53**(2):51-63. https://doi.org/10.1539/joh.l10128
18. Nagano K, Nishizawa T, Umeda Y *et al.* Inhalation carcinogenicity and chronic toxicity of indium-tin oxide in rats and mice. *J Occup Health*. 2011;**53**(3):175-187. https://doi.org/10.1539/joh.10-0057-oa
19. Hiroli PK, Varun S, Sudeep M, Kathik B, Mahendra KS, Manjunatha C. ITO conductive ink: advances in materials, preparation, and potential sensor applications. *ECS Trans*. 2022;**107**(1):20135-20146. https://doi.org/10.1149/10701.20135ecst
20. Matsui H, Shoji M, Higano S *et al.* Infrared plasmonic metamaterials based on transparent nanoparticle films of In_2O_3:Sn for solar-thermal shielding applications. *ACS Appl Mater Interfaces*. 2022;**14**(43):49313-49325. https://doi.org/10.1021/acsami.2c14257
21. Kim BW, Cha W, Choi S, Shin J, Choi BS, Kim M. Assessment of occupational exposure to indium dust for indium-tin-oxide manufacturing workers. *Biomol Ther*. 2021;**11**(3):419. https://doi.org/10.3390/biom11030419
22. Qu J, Wang J, Zhang H *et al.* Toxicokinetics and systematic responses of differently sized indium tin oxide (ITO) particles in mice via oropharyngeal aspiration exposure. *Environ Pollut*. 2021;**290**:117993. https://doi.org/10.1016/j.envpol.2021.117993
23. Liu N, Guan Y, Zhou C, Wang Y, Ma Z, Yao S. Pulmonary and systemic toxicity in a rat model of pulmonary alveolar proteinosis induced by indium-tin oxide nanoparticles. *Int J Nanomedicine*. 2022;**17**:713-731. https://doi.org/10.2147/IJN.S338955
24. Guan Y, Liu N, Yu Y *et al.* Pathological comparison of rat pulmonary models induced by silica nanoparticles and indium-tin oxide nanoparticles. *Int J Nanomedicine*. 2022;**17**:4277-4292. https://doi.org/10.2147/IJN.S380259
25. Tabei Y, Sonoda A, Nakajima Y *et al.* In vitro evaluation of the cellular effect of indium tin oxide nanoparticles using the human lung adenocarcinoma A549 cells. *Metallomics*. 2015;**7**(5):816-827. https://doi.org/10.1039/c5mt00031a
26. Ahmed S, Kobayashi H, Afroz T *et al.* Nitrative DNA damage in lung epithelial cells exposed to indium nanoparticles and indium ions. *Sci Rep*. 2020;**10**(1):10741. https://doi.org/10.1038/s41598-020-67488-3
27. Suzuki T, Sakata S, Makino Y *et al.* iQuant2: software for rapid and quantitative imaging using laser ablation-ICP mass spectrometry. *Mass Spectrom*. 2018;**7**(1):A0065. https://doi.org/10.5702/massspectrometry.A0065
28. Yamashita S, Yoshikuni Y, Obayashi H, Suzuki T, Green D, Hirata T. Simultaneous determination of size and position of silver and gold nanoparticles in onion cells using laser ablation-ICP-MS. *Anal Chem*. 2019;**91**(7):4544-4551. https://doi.org/10.1021/acs.analchem.8b05632
29. Sun H, Li H, Sadler PJ. Transferrin as a metal ion mediator. *Chem Rev*. 1999;**99**(9):2817-2842. https://doi.org/10.1021/cr980430w
30. Van Hulle M, De Cremer K, Cornelis R, Lameire N. *In vivo* distribution and speciation of $[^{114m}In]InCl_3$ in the Wistar rat. *J Environ Monit*. 2001;**3**(1):86-90. https://doi.org/10.1039/B006870P
31. Huaux F, De Gussem V, Lebrun A *et al.* New interplay between interstitial and alveolar macrophages explains pulmonary alveolar proteinosis (PAP) induced by indium tin oxide particles. *Arch Toxicol*. 2018;**92**(4):1349-1361. https://doi.org/10.1007/s00204-018-2168-1
32. Woods JS, Fowler BA. Selective inhibition of δ-aminolevulinic acid dehydratase by indium chloride in rat kidney: biochemical and ultrastructural studies. *Exp Mol Pathol*. 1982;**36**(3):306-315. https://doi.org/10.1016/0014-4800(82)90060-0
33. Castronovo FP, Wagner HN. Factors affecting the toxicity of the element indium. *Br J Exp Pathol*. 1971;**52**(5):543-559
34. Hard GC, Khan KN. A contemporary overview of chronic progressive nephropathy in the laboratory rat, and its significance for human risk assessment. *Toxicol Pathol*. 2004;**32**(2):171-180. https://doi.org/10.1080/01926230490422574